Journal of Experimental Botany, Vol. 66, No. 10 pp. 2967–2977, 2015
doi:10.1093/jxb/erv035 Advance Access publication 5 March 2015

RESEARCH PAPER

ALTERNATIVE OXIDASE1a modulates the oxidative challenge during moderate Cd exposure in *Arabidopsis thaliana* leaves

Els Keunen[1], Kerim Schellingen[1], Dominique Van Der Straeten[2], Tony Remans[1], Jan Colpaert[1], Jaco Vangronsveld[1] and Ann Cuypers[1,*]

[1] Environmental Biology, Centre for Environmental Sciences, Hasselt University, Agoralaan Building D, B-3590 Diepenbeek, Belgium
[2] Laboratory of Functional Plant Biology, Ghent University, Karel Lodewijk Ledeganckstraat 35, B-9000 Ghent, Belgium

* To whom correspondence should be addressed. E-mail: ann.cuypers@uhasselt.be

Received 21 November 2014; Revised 9 January 2015; Accepted 12 January 2015

Abstract

This study aims to unravel the functional significance of alternative oxidase1a (AOX1a) induction in *Arabidopsis thaliana* leaves exposed to cadmium (Cd) by comparing wild-type (WT) plants and *aox1a* knockout mutants. In the absence of AOX1a, differences in stress-responsive transcript and glutathione levels suggest an increased oxidative challenge during moderate (5 µM) and prolonged (72 h) Cd exposure. Nevertheless, *aox1a* knockout leaves showed lower hydrogen peroxide (H_2O_2) accumulation as compared to the WT due to both acute (24 h) and prolonged (72 h) exposure to 5 µM Cd, but not to 10 µM Cd. Taken together, we propose a working model where AOX1a acts early in the response to Cd and activates or maintains a mitochondrial signalling pathway impacting on cellular antioxidative defence at the post-transcriptional level. This fine-tuning pathway is suggested to function during moderate (5 µM) Cd exposure while being overwhelmed during more severe (10 µM) Cd stress. Within this framework, ethylene is required – either directly or indirectly via NADPH oxidase isoform C – to fully induce *AOX1* expression. In addition, reciprocal crosstalk between these components was demonstrated in leaves of *A. thaliana* plants exposed to Cd.

Key words: Alternative oxidase, alternative respiration, *Arabidopsis thaliana*, cadmium (Cd), ethylene, oxidative challenge.

Introduction

In the plant mitochondrial electron transport chain (ETC), two terminal oxidases are able to reduce O_2 to H_2O. In contrast to cytochrome c oxidase (complex IV), the alternative oxidase (AOX) does not translocate protons across the inner membrane. As AOX bypasses proton-pumping complexes III and IV, the energy (ATP) yield is reduced (Millar *et al.*, 2011). Under normal conditions, AOX is suggested to modulate the production of reactive oxygen species (ROS), although conflicting results appear in the literature (Vanlerberghe *et al.*, 2009). Amirsadeghi *et al.* (2006) have reported diminished steady-state cellular ROS levels in tobacco leaves lacking AOX as compared to wild-type (WT) leaves. However, Cvetkovska and Vanlerberghe (2012) demonstrated that a lack of AOX increases superoxide ($O_2^{\bullet-}$) levels in tobacco leaf mitochondria. Nevertheless, these data support the long-standing hypothesis that AOX modulates the production of mitochondrial ROS in plants (Purvis and Shewfelt, 1993).

The relationship between ROS and AOX might also imply a function for this enzyme during abiotic stress conditions, supported by the fact that expression of the dominant *AOX1a* isoform in *Arabidopsis thaliana* is highly stress-responsive (Clifton *et al.*, 2005; Vanlerberghe *et al.*, 2009). Abiotic stress is often characterized by an oxidative challenge at the cell and organelle level (Apel and Hirt, 2004). For example, exposure

Abbreviations: AOX, alternative oxidase; Cd, cadmium; ETC, electron transport chain; GSH, glutathione; GSSG, glutathione disulfide; H_2O_2, hydrogen peroxide; $O_2^{\bullet-}$, superoxide; RBOH, respiratory burst oxidase homologue; ROS, reactive oxygen species.

to cadmium (Cd) is associated with increased ROS generation in plants (Sharma and Dietz, 2009; Cuypers *et al.*, 2011), and mitochondria in particular (Heyno *et al.*, 2008). Moreover, we reported that in the case of Cd exposure, the AOX pathway is activated at the transcriptional and translational level in *A. thaliana* (Keunen *et al.*, 2013). However, the functional implications of AOX induction during Cd stress are still largely unknown.

Similarly to its function, it remains unclear how AOX is induced. Wang *et al.* (2010) have shown that both hydrogen peroxide (H_2O_2) and ethylene are involved in activating alternative respiration in salt-stressed *Arabidopsis* calli. Both ROS (Cuypers *et al.*, 2011) and ethylene (Gallego *et al.*, 2012; Schellingen *et al.*, 2014) are known to mediate Cd stress responses and therefore might also act in the induction and activation of AOX during exposure to Cd.

The current study aims to unravel whether and how AOX modulates Cd stress responses in *A. thaliana*. To this end, WT and *aox1a* knockout plants exposed to sublethal Cd concentrations were compared, and the Cd-induced oxidative challenge was monitored at the transcript and metabolic level in leaves. Moreover, the emerging link between ROS, ethylene and AOX induction and regulation was investigated through a combined reverse genetic approach.

Materials and methods

Plant culture and Cd exposure

WT, *aox1a* knockout (SALK_084897 T-DNA insertional line for *AOX1a*: Alonso *et al.*, 2003; Watanabe *et al.*, 2008), ACC synthase (ACS) *acs2-1/acs6-1* double knockout [N16581 NASC line, defective in Cd-induced ethylene biosynthesis (Schellingen *et al.*, 2014)], and ethylene-insensitive *ein2-1* and *ein2-5* (Alonso *et al.*, 1999) mutant genotypes were confirmed using PCR as described in the above-mentioned papers. All seeds were surface sterilized and hydroponically grown (Smeets *et al.*, 2008), except that purified sand was used instead of rock wool (Keunen *et al.*, 2011). A modified Hoagland nutrient solution was used (Smeets *et al.*, 2008) and growth conditions were set at a 12 h photoperiod, 65% relative humidity and day/night temperatures of 22 and 18°C, respectively. Light was provided by Philips Green-Power LED modules. A combination of blue, red, and far-red modules was used to obtain a spectrum simulating the photosynthetically active radiation (PAR) of sunlight. The PAR provided at the rosette level was 170 µmol m^{-2} s^{-1}. After 19 days of growth, plants were either exposed to 5 or 10 µM $CdSO_4$ supplied to the roots or further grown under control conditions. After 24 and 72 h, leaf (entire rosette) samples were taken and the fresh weight was determined. Samples were snap frozen in liquid nitrogen and stored at –70°C for further analyses, except for Cd content determination (cfr. *infra*; Keunen *et al.*, 2013).

Determination of Cd content and dry weight

At harvest, leaves were rinsed using distilled water. Samples were oven-dried and weighed to determine the dry weight and the percentage of dry weight per plant, calculated as the ratio between dry and fresh weight. Next, samples were digested with 70–71% HNO_3 in a heat block (Cuypers *et al.*, 2002). Concentrations of Cd were determined via inductively coupled plasma–optical emission spectrometry (ICP–OES, Agilent Technologies, 700 Series, Belgium). For reference purposes, blank (HNO_3 only) and standard [NIST Spinach (1570a)] samples were used.

Gene expression analysis

Frozen leaf samples were disrupted in 2 ml microcentrifuge tubes using two stainless steel beads and the Retsch Mixer Mill MM 400 (Retsch, Belgium) under frozen conditions. From the disrupted tissues, RNA was extracted using the RNAqueous® Total RNA Isolation Kit (Ambion, Life Technologies, Belgium). Concentration and purity of the isolated RNA were assessed using the NanoDrop® ND-1000 spectrophotometer (ThermoScientific, USA). To remove any contaminating genomic DNA, equal amounts (1 µg) of the extracted RNA samples were subjected to a DNase treatment using the TURBO DNA-*free*™ Kit (Ambion). Treated RNA samples were converted to single stranded cDNA via the PrimeScript™ RT Reagent Kit (Perfect Real Time, TaKaRa Bio Inc., Westburg, The Netherlands). A tenfold dilution of the cDNA was made in 10^{-1} diluted TE buffer (1 mM Tris-HCl, 0.1 mM Na_2-EDTA, pH 8.0) and stored at –20°C.

Quantitative real-time PCR was performed in optical 96-well plates using the 7500 Fast Real-Time PCR System (Applied Biosystems, Life Technologies, Belgium) and the Fast SYBR® Green Master Mix (Applied Biosystems) according to the manufacturer's instructions. Amplification occurred at universal cycling conditions (20 s at 95°C, 40 cycles of 3 s at 95°C and 30 s at 60°C) followed by the generation of a dissociation curve to verify amplification specificity. Gene-specific forward and reverse primers (300 nM unless stated otherwise; Supplementary Table S1) were designed and optimized via the Primer Express software (v2.0, Applied Biosystems).

Gene expression levels were calculated via the $2^{-\Delta Cq}$ method relative to the sample with the highest expression (minimum Cq). All data were normalized to the expression of three stable reference genes (Remans *et al.*, 2008) selected by geNorm (v3.5; Vandesompele *et al.*, 2002) and Normfinder (v0.953; Andersen *et al.*, 2004) algorithms. Data were normalized using the geometric average of the $2^{-\Delta Cq}$ values for *AT2G28390* (SAND family), *AT4G34270* (TIP41-like), and *AT5G25760* (UBC). All details of the workflow according to the Minimum Information for publication of Quantitative real-time PCR Experiments (MIQE) guidelines as described by Bustin *et al.* (2009) are shown in Supplementary Table S2.

Hierarchical clustering of gene expression data

To identify potential sample-related patterns during Cd exposure in WT versus *aox1a* knockout leaves, hierarchical clustering analysis was performed using GenEx software (v6, MultiD Analyses AB, Sweden). This analysis was based on raw gene expression values and the 'average linkage' algorithm, defining the distance between groups/treatments as the average of distances between all pairs of individuals in all groups. Distances between the measures were calculated via the Euclidian Distance Measure. Heat maps were constructed to compare expression levels between different genes and samples.

In situ *detection of H_2O_2 using 3,3'-diaminobenzidine*

Leaves were stained using 3,3'-diaminobenzidine (DAB) as described by Daudi *et al.* (2012). After DAB oxidation by H_2O_2, an insoluble brown precipitate reflects the presence and tissue distribution of H_2O_2. Leaves (three per plant, six biological replicates per condition) were incubated in 3 ml freshly prepared staining solution [DAB (1 mg ml^{-1}) and Tween-20 (0.05% v/v) in 10 mM Na_2HPO_4, pH 3.0] or control solution (10 mM Na_2HPO_4) using 12-well microtitre plates. As DAB is light-sensitive, all plates were covered using aluminium foil. To improve DAB infiltration into the leaves, a vacuum was applied for 5 min using a desiccator. After shaking the plates at 80 rpm for 4 h, all solutions were replaced by 3 ml bleaching solution [ethanol:acetic acid:glycerol, 3:1:1 (v:v:v)]. After incubation at 95°C for 15 min, the bleaching solution was refreshed, allowed to incubate at room temperature for 30 min and finally stored at 4°C. The following day, leaves were observed under white light using a binocular microscope. Photographs were obtained using a digital camera and

BTV-pro software (Bensoftware). Experiments were repeated twice using independent biological replicates and representative pictures are depicted.

Determination of glutathione content and redox state

Contents of oxidized (GSSG) and reduced (GSH) forms of glutathione were spectrophotometrically determined using the plate reader method previously described by Queval and Noctor (2007). Frozen leaf samples (100 mg) were thoroughly ground in liquid nitrogen using a cooled mortar and pestle. Sample powders were homogenized in 200 mM HCl (800 µl per 120 mg fresh sample weight) and centrifuged for 10 min (16 000*g*, 4°C). Samples were adjusted to pH 4.5 and kept at 4°C during the entire procedure unless specifically mentioned otherwise. Measurement of GSH and GSSG is based on the reduction of 5,5-dithiobis(2-nitrobenzoic acid) (DTNB, 600 µM) by the action of glutathione reductase (GR, 1U ml^{-1}) in the presence of NADPH (500 µM), which was spectrophotometrically monitored at 412 nm for 5 min. Total glutathione concentrations (GSH + GSSG) were calculated relative to a standard curve ranging from 0 to 500 pmol GSH. To determine oxidized GSSG amounts, samples were first incubated with 2-vinyl-pyridine (2-VP, 1% v/v) to precipitate all free GSH present in the sample during 30 min at room temperature. Samples were centrifuged twice (16 000g, 4°C) to precipitate 2-VP prior to the measurement. For quantification purposes, a GSSG standard curve ranging from 0 to 100 pmol was incubated with 2-VP and measured in duplicate concurrently with the samples. Reduced GSH concentrations were derived by subtracting oxidized GSSG from total levels (Queval and Noctor, 2007).

Statistical analyses

All datasets were statistically analysed with ANOVA and the Tukey-Kramer post-hoc test to correct for multiple comparison using R version 2.13.1 (R Development Core Team, 2011). Both normality and homoscedasticity were checked; transformations were applied when necessary to approximate normality. If normality could not be reached, a non-parametric Kruskal-Wallis test, followed by the Wilcoxon rank sum test, was used to determine statistical significance of the data. Outliers were determined using extreme studentized deviate analysis (GraphPad Software, Inc.) at significance level 0.05. The statistical analysis used is indicated in the caption of each table or figure.

For gene expression data, normalized relative quantities were log transformed prior to statistical analysis (Supplementary Table S2). Both differences within and between genotypes (Supplementary Table S3) and overall genotype × treatment interaction effects (Supplementary Table S4) are discussed for each time point. Significant interaction effects depict genes where treatment (Cd) effects differ between both genotypes.

Results

Responses of WT versus *aox1a* knockout plants were compared after 24 and 72 h of exposure to 5 or 10 µM Cd. Both concentrations were previously demonstrated to be sublethal for the WT (Keunen *et al.*, 2011). The two time points were selected based on our kinetic study in Cd-exposed WT plants, where *AOX1a* expression peaked after 24 h and was still enhanced after 72 h Cd exposure in the leaves (Keunen *et al.*, 2013).

Growth parameters and Cd uptake

After 24 h, no significant changes in leaf fresh weight were observed for WT or *aox1a* knockout plants (Table 1A and B). Significant decreases in fresh weight as compared to leaves of unexposed plants were only apparent after 72 h of Cd exposure in both genotypes (Table 1A and B). In general, changes in leaf fresh weight were mirrored by the impact of Cd on dry weight (Table 1C) and dry weight percentages (Table 1D) in a dose-dependent manner after 72 h in both genotypes.

The rise in Cd content in the leaves was correlated with the Cd concentration applied to the nutrient solution, without any significant differences depending on the genotype (Table 2).

Table 1. *Weight parameters of leaves harvested from wild-type (WT) and* aox1a *knockout* A. thaliana *plants*

	24 h		72 h	
	WT	*aox1a*	WT	*aox1a*
A. Fresh weight (mg plant^{-1})				
Control	60.08 ± 2.31^{a}	55.12 ± 2.97^{a}	100.84 ± 2.94^{a}	89.98 ± 4.64^{a}
5 µM Cd	57.20 ± 2.62^{a}	55.70 ± 0.72^{a}	73.45 ± 4.28^{b}	67.06 ± 3.01^{b,d}
10 µM Cd	54.30 ± 2.76^{a}	56.36 ± 1.84^{a}	46.93 ± 3.22^{c}	52.69 ± 2.48^{c,d}
B. Growth inhibition relative to control (%)				
Control	0.00^{a}	0.00^{a}	0.00^{a}	0.00^{a}
5 µM Cd	4.79^{a}	0.00^{a}	27.16^{b,d}	25.47^{b}
10 µM Cd	9.61^{a}	0.00^{a}	53.46^{c}	41.44^{c,d}
C. Dry weight (mg plant^{-1})				
Control	5.38 ± 0.27^{a}	4.87 ± 0.25^{a}	8.80 ± 0.24^{a}	7.86 ± 0.41^{a,b}
5 µM Cd	5.33 ± 0.18^{a}	5.18 ± 0.06^{a}	7.92 ± 0.35^{a,b}	7.28 ± 0.22^{a,b}
10 µM Cd	5.35 ± 0.31^{a}	5.55 ± 0.22^{a}	6.55 ± 0.49^{b}	7.19 ± 0.39^{b}
D. Dry weight plant^{-1} (%)				
Control	8.95 ± 0.12^{a}	8.85 ± 0.13^{a}	8.73 ± 0.08^{a}	8.74 ± 0.07^{a}
5 µM Cd	9.35 ± 0.18^{a,b}	9.30 ± 0.09^{a,b}	10.82 ± 0.36^{b}	10.90 ± 0.32^{b}
10 µM Cd	9.83 ± 0.11^{b}	9.85 ± 0.12^{b}	13.99 ± 0.60^{c}	13.68 ± 0.58^{c}

All parameters were determined for 19-days-old plants exposed to 5 or 10 µM $CdSO_4$ for 24 and 72 h or grown under control conditions. Data are given as the mean ± SE of five biological replicates, each consisting of at least 10 individual rosettes. Different letters represent significant differences within and between both genotypes ($P < 0.05$), tested within each exposure time (two-way ANOVA). WT, wild-type; *aox1a*, *aox1a* knockout.

Connection between AOX1a and the Cd-induced oxidative challenge in A. thaliana leaves

When comparing WT and *aox1a* knockout plants, it is worth noting that transcript levels of all measured genes (except for *AOX1a*) did not differ between unexposed genotypes. We previously demonstrated that sublethal Cd exposure activates the mitochondrial alternative ETC at the transcript level in *A. thaliana* WT leaves (Keunen *et al.*, 2013). In this research, it was demonstrated that only *AOX1a* and *AOX1d* are expressed and increased upon Cd exposure in the leaves under our experimental conditions. In the present study, *AOX1a* transcript levels significantly peaked after 24 h exposure to both Cd concentrations in the WT (Fig. 1A). Without functional AOX1a, transcript levels of *AOX1d* increased to a greater extent after prolonged (72 h) exposure to 5 and 10 µM Cd in the leaves as compared to the WT (Fig. 1B).

Although genotype-dependent differences were observed for *AOX1a* and *AOX1d* expression, Cd-induced changes in expression of alternative ETC components such as alternative NAD(P)H dehydrogenases (NDs) and uncoupling proteins (UCPs) (Keunen *et al.*, 2013) were generally similar in both WT and *aox1a* knockout leaves (Supplementary Table S3). However, a significant overall genotype × treatment interaction effect was observed for *UCP5* after 72 h (Supplementary Table S4), indicating that the treatment effect differs between both genotypes. Indeed, expression levels of this gene were higher in *aox1a* knockout than in WT leaves from plants exposed to 5 µM Cd for 72 h (Supplementary Table S3).

Gadjev *et al.* (2006) have described a set of five transcripts that were upregulated more than fivefold in different experimental conditions eliciting oxidative stress. These genes are now collectively referred to as hallmarks for general oxidative stress, independent of the ROS type or where ROS are produced (Gadjev *et al.*, 2006). Transcript levels of all hallmark genes were increased in WT and *aox1a* knockout plants upon Cd exposure (Fig. 1C–G). It should be noted, however, that overall genotype × treatment interaction effects were significant for three markers after 72 h (Supplementary Table S4). Transcript levels of the 'upregulated by oxidative stress' gene (*UPOX*, *AT2G21640*), expressed in plant mitochondria (Sweetlove *et al.*, 2002), were used to estimate the extent of the mitochondrial oxidative challenge induced by Cd. A clear genotype-dependent effect was detected as *UPOX* expression was upregulated to a higher level after 72 h exposure to 5 µM Cd in *aox1a* knockout in comparison to WT leaves (Fig. 1C). Similar results were obtained for the unknown *AT1G19020* (Fig. 1E) and TIR-class gene (*AT1G57630*, Fig. 1G).

To further characterize the Cd-induced oxidative challenge at the metabolic level, H_2O_2 production and GSH concentrations and redox state were determined. In both genotypes, Cd exposure increased the presence of DAB precipitates after 24 and 72 h (Fig. 2). However, the leaves of *aox1a* knockout plants exposed to 5 µM Cd showed less intense staining as compared to WT plants (Fig. 2, middle row panels), suggesting a lower production of H_2O_2 under these conditions. Concerning the concentrations and redox state of GSH (Table 3), a markedly lower GSSG content was observed for WT and *aox1a* knockout plants after 24 h exposure to 5 or 10 µM Cd as compared to control conditions. Consequently, a more reduced redox state was apparent (Table 3). After 72 h, GSSG levels rose at 10 µM Cd, however only significantly in *aox1a* knockout mutants, but without significant alteration of the redox state (Table 3). Reduced and total GSH levels significantly increased in 5 µM Cd-exposed WT plants after 72 h. This was not observed in *aox1a* knockout mutants (Table 3). However, exposure to 10 µM Cd caused similar increases in GSH levels in both WT and *aox1a* knockout leaves (Table 3).

Transcriptional alterations in ROS-producing and -scavenging components

Exposure to Cd affects transcript levels of genes encoding ROS-producing and -scavenging proteins (Cuypers *et al.*, 2011; Jozefczak *et al.*, 2014). In this study, our aim was to determine whether and how AOX1a affects the Cd-induced oxidative challenge at the transcript level in *A. thaliana* leaves. Therefore, relative expression levels of different ROS-producing genes and both mitochondrial and other ROS-scavenging genes (Supplementary Table S1) were determined in WT and *aox1a* knockout plants exposed to 5 or 10 µM Cd for 24 and 72 h (Supplementary Tables S3 and S4). In general, for WT plants, responses corresponded with our earlier work as described by Cuypers *et al.* (2011), Keunen *et al.* (2013) and Jozefczak *et al.* (2014). Expression levels of ROS-producing lipoxygenases and antioxidative genes such as catalase isoforms 1 and 3 and glutathione reductase 1 were increased after Cd exposure. Moreover, the Cd-mediated decrease in copper/zinc superoxide dismutase expression was confirmed (Supplementary Table S3). When comparing WT and *aox1a* knockout plants, it is worthwhile noting that

Table 2. *Cadmium content of leaves harvested from wild-type (WT) and* aox1a *knockout* A. thaliana *plants*

	24 h		72 h	
	WT	*aox1a*	WT	*aox1a*
Control	nd	nd	nd	nd
5 µM Cd	799.25 ± 47.01[a]	803.66 ± 24.94[a]	1440.93 ± 78.58[a]	1578.63 ± 61.63[a]
10 µM Cd	1441.17 ± 115.12[b]	1284.11 ± 117.28[b]	2027.68 ± 138.17[b]	2273.63 ± 106.61[b]

Cadmium levels (mg kg^{-1} dry weight) were determined in 19-days-old plants exposed to 5 or 10 µM $CdSO_4$ for 24 and 72 h or grown under control conditions. Data are given as the mean ± SE of five biological replicates. No Cd could be detected in unexposed plants (nd). Different letters represent significant differences within and between both genotypes ($P < 0.05$), tested within each exposure time (two-way ANOVA). WT, wild-type; *aox1a*, *aox1a* knockout.

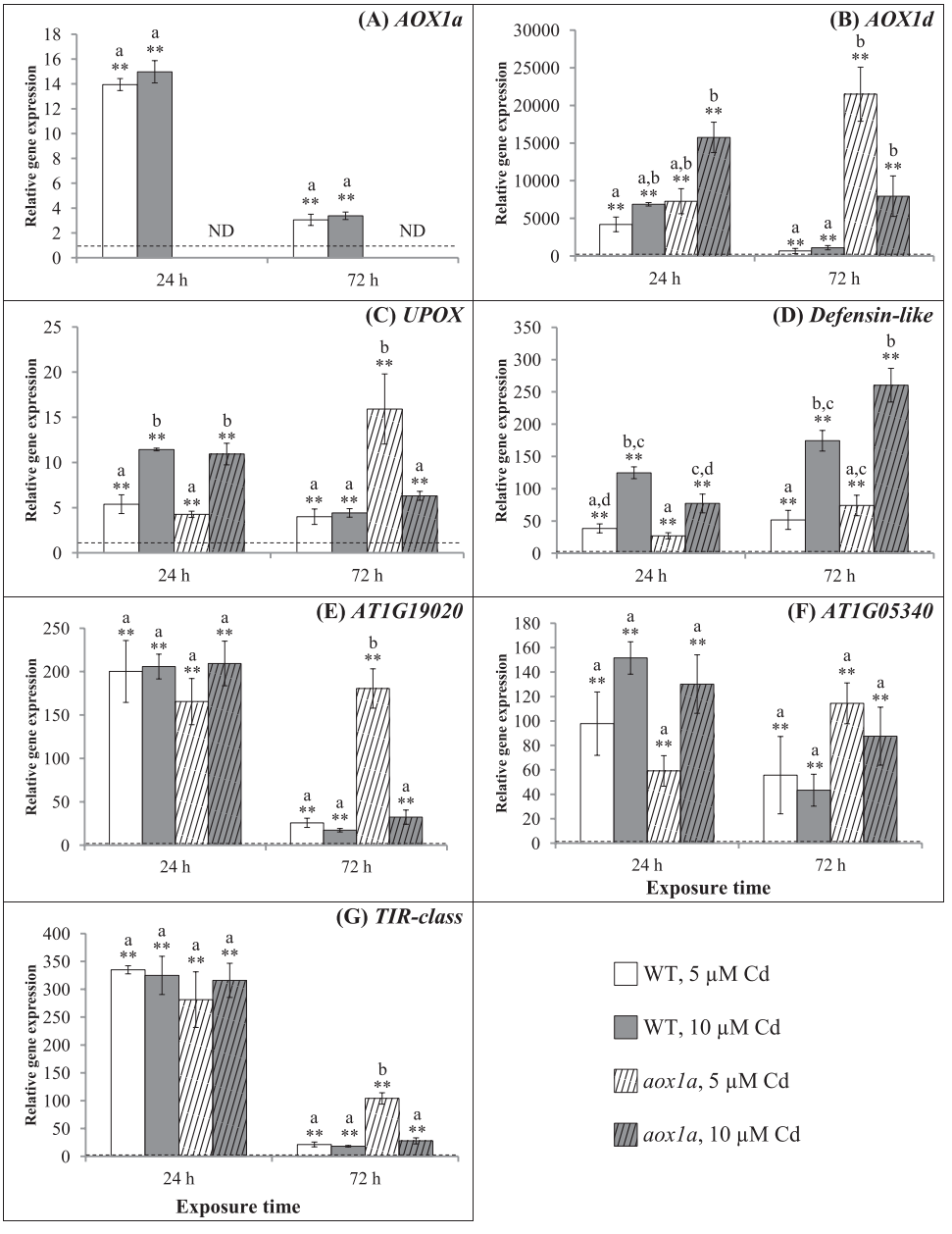

Fig. 1. Relative leaf transcript levels of *AOX1a* (A), *AOX1d* (B), and the oxidative stress hallmark genes (C–G) in *A. thaliana*. Transcript levels were measured via quantitative real-time PCR in leaf samples of 19-days-old WT and *aox1a* knockout (*aox1a*) plants exposed to 5 or 10 µM $CdSO_4$ for 24 and 72 h or grown under control conditions. Per time point, data are given as the mean ± SE of four biological replicates relative to the unexposed genotype set at 1.00 (dashed line). Within each genotype and time point, significant Cd-induced expression changes relative to the control are indicated by asterisks: **, $P < 0.01$. Different letters denote significant differences within and between both genotypes ($P < 0.05$), tested within each exposure time (two-way ANOVA). *AOX*, alternative oxidase; *UPOX*, upregulated by oxidative stress; *TIR*, *Toll-Interleukin-1*.

transcript levels of all measured genes did not differ between unexposed genotypes. Although Cd-induced expression changes were generally similar in both genotypes, a significant genotype × treatment interaction effect was observed for the respiratory burst oxidase homologue C (*RBOHC*) gene after prolonged (72 h) Cd exposure (Supplementary Table S4). Indeed, *RBOHC* expression levels increased to a greater extent in *aox1a* knockout as compared to WT plants after 72 h exposure to 5 µM Cd (Supplementary Table S3).

Hierarchical clustering analysis including all samples and all measured genes (Supplementary Table S1) was performed for both genotypes (Fig. 3). Control samples clustered apart from Cd-exposed samples in the WT as well as *aox1a* mutant plants. In WT leaves, Cd-exposed samples were generally grouped per time point (24 and 72 h) independent of the Cd concentration applied (Fig. 3A). While the same held true for Cd-exposed samples after 24 h in *aox1a* knockout mutants, a separate clustering of 5 and 10 µM Cd-exposed samples occurred after 72 h in the absence of AOX1a (Fig. 3B).

Mechanistic insights into AOX induction and regulation in leaves of Cd-exposed A. thaliana *plants*

Ethylene is undoubtedly involved in Cd-induced signalling as recently evidenced by Schellingen *et al.* (2014). Moreover, ethylene and/or ROS are potentially involved in modulating

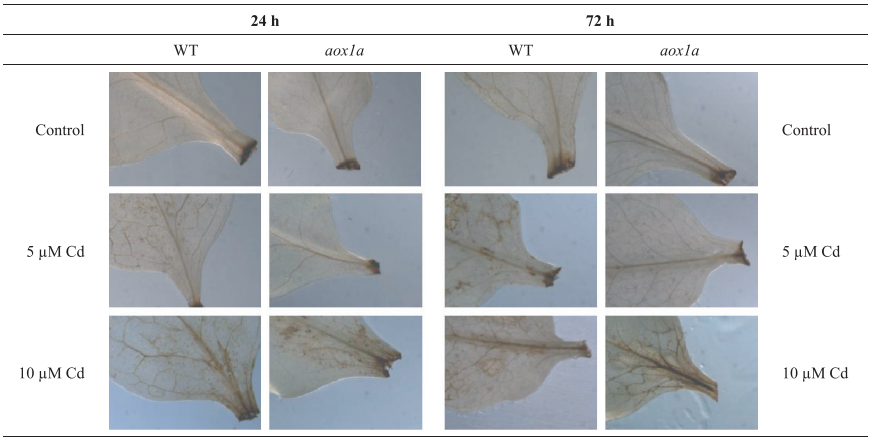

Fig. 2. Production of H_2O_2 as detected by DAB in the leaves. Staining was performed using leaves of WT and *aox1a* knockout (*aox1a*) *A. thaliana* plants either exposed to 5 or 10 µM $CdSO_4$ for 24 and 72 h or grown under control conditions. Per condition, three rosette leaves of six biological replicates were sampled, and representative photographs from two independent experiments are depicted here.

Table 3. *Leaf glutathione concentrations and redox state*

		24 h		72 h	
		WT	*aox1a*	WT	*aox1a*
Total GSH + GSSG	**Control**	223.53 ± 12.86	210.48 ± 15.78	171.03 ± 9.31	173.22 ± 5.82
	5 µM Cd	194.31 ± 25.34	201.80 ± 13.37	312.34 ± 25.31**	254.95 ± 29.83
	10 µM Cd	257.82 ± 15.06	218.30 ± 16.92	397.90 ± 43.90**	456.04 ± 36.92**
GSH	**Control**	216.76 ± 13.10	197.37 ± 15.33	162.39 ± 9.50	166.03 ± 5.98
	5 µM Cd	193.51 ± 25.39	197.47 ± 12.04	305.14 ± 24.42**	246.69 ± 30.30
	10 µM Cd	255.14 ± 14.50	213.39 ± 17.01	381.01 ± 43.94**	445.86 ± 36.00**
GSSG	**Control**	6.77 ± 1.60	13.10 ± 1.51	8.64 ± 1.41	5.15 ± 0.65
	5 µM Cd	0.80 ± 0.11*	0.94 ± 0.20**	7.20 ± 1.66	8.26 ± 1.13
	10 µM Cd	2.68 ± 1.22	4.91 ± 1.02**	16.89 ± 4.41	10.18 ± 1.31*
GSSG / GSH	**Control**	0.032 ± 0.008	0.067 ± 0.008	0.054 ± 0.010	0.031 ± 0.005
	5 µM Cd	0.005 ± 0.001*	0.005 ± 0.001**	0.023 ± 0.005	0.037 ± 0.008
	10 µM Cd	0.010 ± 0.005	0.024 ± 0.006**	0.048 ± 0.013	0.023 ± 0.002

Total GSH levels (nmol GSH equivalents g^{-1} fresh weight) consist of both reduced (GSH) and oxidized glutathione disulfide (GSSG), thereby also determining the ratio between oxidized and reduced forms (*i.e.* the redox state). Concentrations were determined in leaves of 19-days-old WT and *aox1a* knockout (*aox1a*) *A. thaliana* plants exposed to 5 or 10 µM $CdSO_4$ for 24 and 72 h or grown under control conditions. Data are given as the mean ± SE of at least four biological replicates. Per time point, significant Cd-induced changes within a genotype are indicated by (*) ($P < 0.05$) or (**) ($P < 0.01$) (one-way ANOVA).

AOX upregulation during stress (Wang *et al.*, 2010; Li *et al.*, 2013). To further strengthen the emerging link between ethylene, ROS and AOX, we used a reverse genetic approach combining ethylene biosynthesis (*acs2-1/6-1* knockout), ethylene signalling (*ein2-1*) and *aox1a* knockout mutants. Based on the increased induction of the oxidative stress hallmark genes in leaves of 5 µM Cd-exposed *aox1a* knockout as compared to WT plants, all genotypes were exposed to 5 µM Cd for 24 and 72 h. Transcript levels were compared between different genotypes and expressed relative to their own control (Fig. 4). Under control conditions, expression levels of *AOX1a*, *AOX1d* and *RBOHC* were significantly higher in *ein2-1* mutants as compared to the WT, albeit only after 24 h (Supplementary Table S5). Upregulation of *AOX1a* (Fig. 4A) and *AOX1d* (Fig. 4B) was significantly lower in leaves of both ethylene mutants exposed to 5 µM Cd as compared to WT plants. Moreover, *RBOHC* upregulation was weaker or even absent in Cd-exposed *acs2-1/6-1* and *ein2-1* mutants (Fig. 4C). Similar results were obtained for the leaves of 5 µM Cd-exposed *ein2-5* mutants (Supplementary Figure S1).

After 72 h exposure to 5 µM Cd, transcript levels of *RBOHC* were higher in *aox1a* knockout leaves as compared to the WT (Fig. 4D). Similarly, expression of the ethylene biosynthesis ACC synthase 6 (*ACS6*, Fig. 4E) and ethylene receptor 2 (*ETR2*, Fig. 4F) genes was induced to a greater extent under the same conditions. Both observations point towards a regulatory role of AOX1a in the upregulation of *RBOHC* and genes involved in ethylene synthesis and signalling (middle scheme in Fig. 4). For the sake of completeness, transcript levels of ethylene biosynthesis as well as signal transduction genes (Supplementary Table S1) were determined in WT and *aox1a* knockout plants, also after exposure to 10 µM Cd (Supplementary Table S3). In general, most differences observed between both genotypes after prolonged (72 h) exposure to 5 µM Cd (Fig. 4) disappeared after

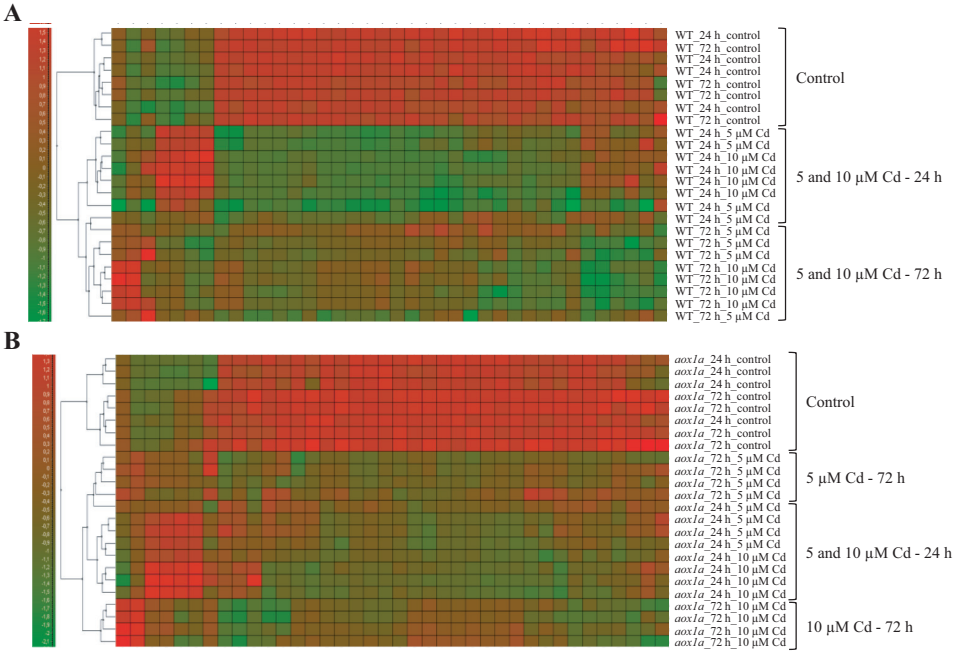

Fig. 3. Hierarchical classification of transcript levels in leaf samples. Results are visualized using dendrograms and heat maps indicating expression levels in the leaves of WT (A) and *aox1a* knockout (B) *A. thaliana* plants. Each column of the map represents a different gene.

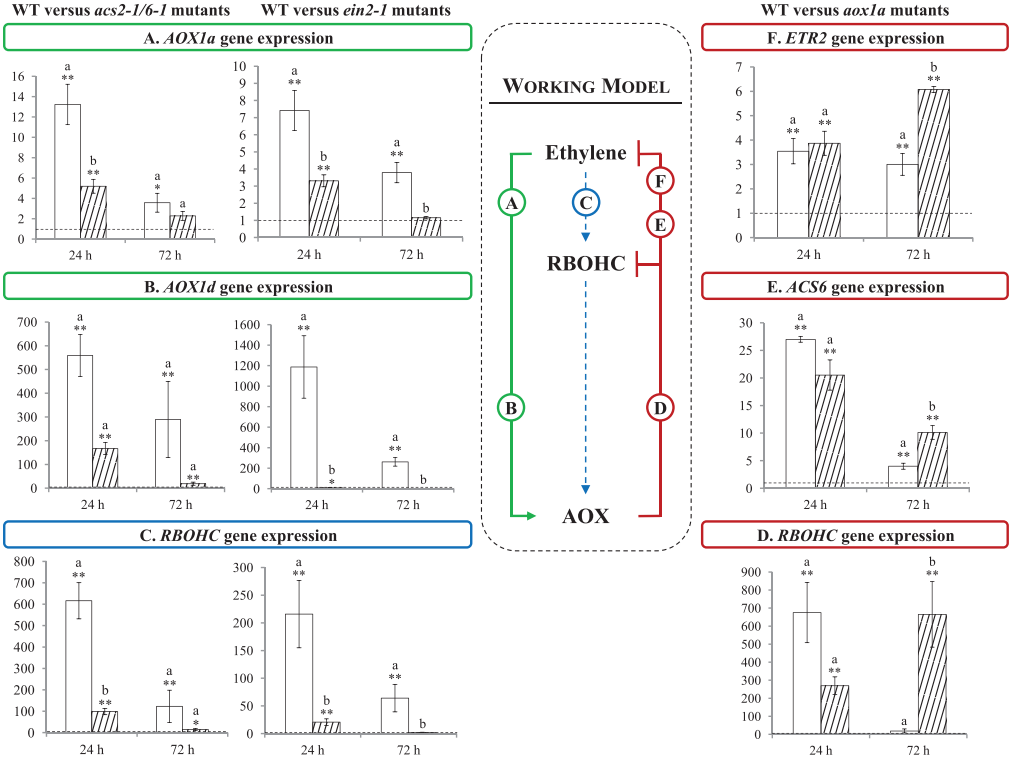

Fig. 4. Schematic overview of the interplay between ethylene, RBOHC and AOX in leaves of Cd-exposed *A. thaliana* plants. Transcript levels were measured via quantitative real-time PCR in leaf samples of 19-days-old WT plants and *acs2-1/acs6-1* double knockout (*acs2-1/6-1*), ethylene-insensitive *ein2-1* or *aox1a* knockout mutants (*aox1a*) exposed to 5 µM $CdSO_4$ (WT, white; mutant, white striped) for 24 and 72 h or grown under control conditions. Per time point, data are given as the mean ± SE of four biological replicates relative to the unexposed genotype set at 1.00 (dashed line). Within each genotype and time point, significant Cd-induced expression changes relative to the control are indicated using asterisks: *, $P < 0.05$; **, $P < 0.01$. Different letters denote significant differences between both genotypes ($P < 0.05$), tested within each exposure time (two-way ANOVA). Expression levels of *AOX1a* (A), *AOX1d* (B) and *RBOHC* (C) were determined in WT, *acs2-1/6-1* and *ein2-1* mutants. Moreover, *RBOHC* (D), *ACS6* (E), and *ETR2* (F) transcript levels were measured in WT and *aox1a* mutants. A working model for the putative interactions between ethylene, RBOHC and AOX is depicted in the middle. *ACS*, ACC synthase; *AOX*, alternative oxidase; *ETR*, ethylene receptor; *RBOHC*, respiratory burst oxidase homologue C.

exposure to the highest Cd concentration (Supplementary Table S3).

Discussion

Previous results indicated that AOX respiration is involved in *A. thaliana* stress responses to Cd at transcript and protein levels (Keunen *et al.*, 2013). In the current work, the significance of AOX induction during moderate (5 µM) and more severe (10 µM) Cd stress was studied by comparing WT and *aox1a* knockout plants. Prior to Cd exposure, no clear phenotypic differences were visible between both genotypes. Corresponding with previous research (Giraud *et al.*, 2008), this supports the view that a lack of AOX has minor to no consequences under non-stress conditions but particularly impacts (abiotic) stress responses (Vanlerberghe *et al.*, 2009). However, Cd content and weight parameters were comparably affected in WT and *aox1a* knockout plants (Tables 1 and 2). Therefore, Cd-induced responses were compared between both genotypes at the molecular level.

A modulating role for AOX1a during the oxidative challenge under moderate (5 µM) Cd exposure

In general, our assessment of the Cd-induced oxidative challenge at transcript and metabolic levels revealed that most differences between WT and *aox1a* knockout plants were occurring under moderate (*i.e.* 5 µM) Cd exposure. For example, expression levels of the oxidative stress hallmark genes *UPOX* (Fig. 1C), *AT1G19020* (Fig. 1E) and the TIR-class gene (Fig. 1G) were induced to a higher extent after 72 h exposure to 5 µM Cd in *aox1a* knockout in comparison to WT leaves. As demonstrated by Cvetkovska and Vanlerberghe (2012), a lack of AOX increases mitochondrial $O_2^{\bullet-}$ production. Therefore, higher *UPOX* upregulation in the absence of AOX1a coincides with an enhanced mitochondrial oxidative challenge under moderate Cd stress. Moreover, a lack of functional AOX1a can have consequences outside mitochondria, as evidenced by the higher upregulation of the chloroplast TIR-class gene in leaves of 5 µM Cd-exposed *aox1a* knockout versus WT plants. Similarly, Giraud *et al.* (2008) reported increases in stress-responsive transcripts and particularly those that encode ROS scavengers in chloroplasts during combined light and drought stress in the absence of AOX1a.

Under normal conditions, it has been shown that AOX-suppressed tobacco leaves have similar to lower H_2O_2 concentrations as compared to WT leaves (Cvetkovska and Vanlerberghe, 2012). Consistently, results in both tobacco (Amirsadeghi *et al.*, 2006) and *Arabidopsis* (Watanabe *et al.*, 2008) point towards induced ROS-scavenging when AOX is missing. Nevertheless, we did not observe differences in DAB staining between WT and *aox1a* knockout leaves under normal growth conditions. During exposure to 5 µM Cd, however, H_2O_2 accumulated to a lesser extent in *aox1a* knockout leaves (Fig. 2). Pasqualini *et al.* (2007) reported that leaves of transgenic tobacco plants overexpressing AOX1a showed increased and persistent H_2O_2 levels during acute ozone fumigation as compared to WT plants. The attenuation of H_2O_2 levels after 24 and 72 h of Cd exposure in our study could have an impact at a more prolonged stage (72 h), for example when comparing GSH responses in both genotypes. The absence of a significant increase in GSH levels in leaves of 5 µM Cd-exposed *aox1a* knockout as compared to WT plants after 72 h (Table 3) coincides with an altered oxidative challenge as evidenced by the hallmark genes (Fig. 1).

Taken together, our data suggest that a lack of functional AOX1a disrupts a signalling pathway emerging from the mitochondrion early after the start of Cd exposure. A role for AOX1a in acute Cd stress responses is underlined by the observed peak in its expression levels after 24 h (Fig. 1A) and its transient increase at the protein level (Keunen *et al.*, 2013). The nature of the retrograde signal initiated by AOX is currently unknown, but ROS are often put forward (Vanlerberghe *et al.*, 2009). In line with this, we suggest the involvement of H_2O_2 as its levels were attenuated in leaves of plants lacking AOX1a during 5 µM Cd exposure. Nevertheless, the role of other signalling metabolites should also be explored as AOX is intimately related to the carbon and nitrogen metabolism under physiological (Gandin *et al.*, 2014) and stress conditions (Watanabe *et al.*, 2008). In addition, it is unclear which cellular functional level is controlled by the AOX1a signalling pathway during Cd stress. Expression levels of genes involved in the ROS network did not change in leaves of *aox1a* knockout versus WT plants (Supplementary Table S3). Therefore, we suggest that the AOX1a signalling pathway regulates defence mechanisms to moderate (5 µM) Cd stress at a post-transcriptional level in *A. thaliana* leaves.

In reverse genetic studies, it is often observed that other components of the alternative respiratory pathway, such as NDs and UCPs, try to compensate for the absence of functional AOX1a. For example, Watanabe *et al.* (2008) have demonstrated increased transcript levels of *NDB2* and *UCP1* isoforms in *A. thaliana* leaves lacking AOX1a as compared to the WT under low temperature. While in our study *ND* and *UCP* genes mostly did not show altered expression levels in the absence of AOX1a (Supplementary Table S3), expression of *AOX1d* was more abundant in leaves of Cd-exposed *aox1a* knockout mutants, again highly pronounced after 72 h exposure to 5 µM Cd (Fig. 1B). Strödtkotter *et al.* (2009) have demonstrated that AOX1d was unable to take over the function of AOX1a in *A. thaliana* exposed to antimycin A. Functional compensation of AOX1a by AOX1d is unlikely in our conditions as well, since *aox1a* knockout mutants did show a differential response to 5 µM Cd as compared to WT plants.

Finally, all differences observed in leaves of 5 µM Cd-exposed *aox1a* knockout as compared to WT plants after 72 h disappeared when comparing responses to the highest Cd concentration. This is supported by our clustering analysis, where leaf samples from 5 µM Cd-exposed mutants clustered separately from those derived from plants exposed to 10 µM Cd at 72 h (Fig. 3). The latter plants severely suffer as indicated by ~50% growth inhibition (Table 1B) and increased total H_2O_2 levels (Fig. 2). The enhanced ROS accumulation did cause oxidative damage, but only after 72 h exposure to the highest Cd concentration (Keunen *et al.*, 2013). Therefore, we hypothesize that the AOX1a signal initiates a fine-tuning pathway that is overwhelmed when stress levels are more

severe (10 µM Cd). Nonetheless, plants are able to survive long-term exposure to 10 µM Cd (Keunen *et al.*, 2011).

The emerging link between ethylene, ROS and AOX in leaves of Cd-exposed A. thaliana *plants*

Recently, more research has been dedicated to unravelling the nature of primary signals that genetically control AOX respiration in plants (Vanlerberghe, 2013). Li *et al.* (2013) have shown that mitochondrial $O_2^{\bullet-}$ modulates rice *AOX1* gene expression under cold, drought and salinity stress. In addition to ROS, ethylene was shown to be implicated in the induction of alternative respiration in salt-treated *Arabidopsis* calli (Wang *et al.*, 2010).

In the current work, we demonstrate the necessity of functional ethylene biosynthesis and signal transduction to fully induce *AOX1* genes in leaves of 5 µM Cd-exposed *A. thaliana* plants (Fig. 4). To this end, we compared transcriptional responses in Cd-exposed WT and *acs2-1/6-1* knockout plants. The use of these mutants is justified as increased expression levels of both *ACS2* and *ACS6* mainly mediate ethylene biosynthesis and responses in Cd-exposed *A. thaliana* plants (Schellingen *et al.*, 2014). In *acs2-1/6-1* knockout mutant leaves, induction of both *AOX1a* and *AOX1d* was lowered as compared to the WT, and this was most pronounced after 24 h exposure to 5 µM Cd. Furthermore, Cd-induced responses were compared between WT plants and *ein2-1* mutants. As EIN2 is a central component in the ethylene-signalling pathway, *ein2-1* mutant lines are completely insensitive to this hormone (Alonso *et al.*, 1999). Under ethylene-insensitive conditions, the induction of *AOX1a* and *AOX1d* by Cd completely disappeared after 72 h (Fig. 4A and B). A similar response was observed for *ein2-5* mutants as compared to the WT (Supplementary Figure S1). A link between ethylene and *AOX1d* induction was also reported by Buchanan-Wollaston *et al.* (2005), who observed diminished upregulation of *AOX1d* in senescing leaves of *ein2-1* mutants as compared to WT plants. Furthermore, AOX was demonstrated to play a regulatory role during ethylene-induced plant cell death (Lei *et al.*, 2003) as well as tomato fruit ripening (Xu *et al.*, 2012). Exposure to Cd is related to accelerated leaf ageing (Sandalio *et al.*, 2001) and ethylene might at least contribute to this response in *A. thaliana* (Schellingen *et al.*, 2014).

Although ethylene induces *AOX1* expression during Cd exposure, other components are also suggested to be involved. Ederli *et al.* (2006) showed that both ethylene-dependent and -independent pathways are required to increase *AOX1a* expression in tobacco plants exposed to ozone. In addition, evidence was presented for the essential role of nitric oxide (NO) as an upstream signalling component activating *AOX*. As NO is suggested to be involved in Cd stress responses as well (Arasimowicz-Jelonek *et al.*, 2011), its role in genetic control of AOX respiration should be addressed in future studies.

It is tempting to speculate about the involvement of ROS and more particularly $O_2^{\bullet-}$ generated by NADPH oxidases (dashed arrows in Fig. 4) in the modulation of *AOX* by ethylene. Jiang *et al.* (2013) have demonstrated that enhanced ethylene production potently promotes salt tolerance in *A. thaliana*, which is correlated with elevated ROS levels and RBOHF function. Moreover, expression of *RBOHD* and *RBOHF* genes is preceded by ethylene biosynthesis in *Brassica oleracea* (Jakubowicz *et al.*, 2010). Upon Cd exposure, expression of *RBOHC*, which was the highest induced isoform in leaves (Remans *et al.*, 2010), did not increase to WT levels in *acs2-1/6-1* knockout, *ein2-1* (Fig. 4C) and *ein2-5* mutants (Supplementary Figure S1). These results clearly link ethylene to ROS production by NADPH oxidases, which might also mediate stress responses inducing *AOX1* genes and leading to signalling and acclimation during moderate (*i.e.* 5 µM Cd) exposure. On the other hand, the involvement of negative feedback mechanisms from AOX to RBOHC/ethylene was demonstrated using *aox1a* knockout plants. Indeed, the induction of *RBOHC* (Fig. 4D), the ethylene biosynthesis gene *ACS6* (Fig. 4E), and ethylene signalling gene *ETR2* (Fig. 4F) was enhanced in the absence of AOX1a. This higher induction correlates with an increased expression level of the oxidative stress hallmark genes in leaves of 5 µM Cd-exposed *aox1a* knockout as compared to WT plants after 72 h (Fig. 1). Taken together, these data suggest reciprocal crosstalk between ethylene, RBOHC and AOX during moderate Cd exposure in *A. thaliana* leaves (Fig. 4).

Supplementary material

Supplementary data can be found at *JXB* online.

Supplementary Table S1. Forward and reverse primers used to determine gene expression levels via quantitative real-time PCR.

Supplementary Table S2. Quantitative real-time PCR parameters according to the MIQE guidelines derived from Bustin *et al.* (2009).

Supplementary Table S3. Relative leaf transcript levels of wild-type and *aox1a* knockout *A. thaliana* plants.

Supplementary Table S4. Overall genotype × treatment interaction effects represented by the *P*-values for all measured genes in wild-type and *aox1a* knockout *A. thaliana* leaves for each time point.

Supplementary Table S5. Relative leaf transcript levels of genes encoding AOXs (*AOX1a* and *AOX1d*) and RBOHC in different genotypes of *A. thaliana* under control conditions.

Supplementary Figure S1. Relative leaf transcript levels of *AOX1a* (A), *AOX1d* (B), and *RBOHC* in wild-type and *ein2-5* mutant *A. thaliana* plants.

Funding

This work was supported by the Research Foundation Flanders (FWO) through a PhD grant for EK and the project [G0D3414]. Additional funding came from Hasselt University through the Methusalem project [08M03VGRJ].

Acknowledgments

We thank Carine Put and Ann Wijgaerts for their skilful technical assistance. Seeds of *aox1a* knockout plants (Columbia ecotype) were kindly provided by Dr Chihiro Watanabe (Department of Biological Sciences, Graduate School of Science, The University of Tokyo, Japan).

References

Alonso JM, Hirayama T, Roman G, Nourizadeh S, Ecker JR. 1999. EIN2, a bifunctional transducer of ethylene and stress responses in *Arabidopsis*. *Science* **284,** 2148–2152.

Alonso JM, Stepanova AN, Leisse TJ, *et al*. 2003. Genome-wide insertional mutagenesis of *Arabidopsis thaliana*. *Science* **301,** 653–657.

Amirsadeghi S, Robson CA, McDonald AE, Vanlerberghe GC. 2006. Changes in plant mitochondrial electron transport alter cellular levels of reactive oxygen species and susceptibility to cell death signaling molecules. *Plant and Cell Physiology* **47,** 1509–1519.

Andersen CL, Jensen JL, Ørntoft TF. 2004. Normalization of real-time quantitative reverse transcription-PCR data: A model-based variance estimation approach to identify genes suited for normalization, applied to bladder and colon cancer data sets. *Cancer Research* **64,** 5245–5250.

Apel K, Hirt H. 2004. Reactive oxygen species: Metabolism, oxidative stress, and signal transduction. *Annual Review of Plant Biology* **55,** 373–399.

Arasimowicz-Jelonek M, Floryszak-Wieczorek J, Gwóźdź EA. 2011. The message of nitric oxide in cadmium challenged plants. *Plant Science* **181,** 612–620.

Buchanan-Wollaston V, Page T, Harrison E, *et al*. 2005. Comparative transcriptome analysis reveals significant differences in gene expression and signalling pathways between developmental and dark/starvation-induced senescence in Arabidopsis. *The Plant Journal* **42,** 567–585.

Bustin SA, Benes V, Garson JA, *et al*. 2009. The MIQE guidelines: Minimum Information for publication of Quantitative real-time PCR Experiments. *Clinical Chemistry* **55,** 611–622.

Clifton R, Lister R, Parker KL, Sappl PG, Elhafez D, Millar AH, Day DA, Whelan J. 2005. Stress-induced co-expression of alternative respiratory chain components in *Arabidopsis thaliana*. *Plant Molecular Biology* **58,** 193–212.

Cuypers A, Smeets K, Ruytinx J, *et al*. 2011. The cellular redox state as a modulator in cadmium and copper responses in *Arabidopsis thaliana* seedlings. *Journal of Plant Physiology* **168,** 309–316.

Cuypers A, Vangronsveld J, Clijsters H. 2002. Peroxidases in roots and primary leaves of *Phaseolus vulgaris*. Copper and zinc phytotoxicity: a comparison. *Journal of Plant Physiology* **159,** 869–876.

Cvetkovska M, Vanlerberghe GC. 2012. Alternative oxidase modulates leaf mitochondrial concentrations of superoxide and nitric oxide. *New Phytologist* **195,** 32–39.

Daudi A, Cheng Z, O'Brien JA, Mammarella N, Khan S, Ausubel FM, Bolwell GP. 2012. The apoplastic oxidative burst peroxidase in *Arabidopsis* is a major component of pattern-triggered immunity. *The Plant Cell* **24,** 275–287.

Ederli L, Morettini R, Borgogni A, Wasternack C, Miersch O, Reale L, Ferranti F, Tosti N, Pasqualini S. 2006. Interaction between nitric oxide and ethylene in the induction of alternative oxidase in ozone-treated tobacco plants. *Plant Physiology* **142,** 595–608.

Gadjev I, Vanderauwera S, Gechev TS, Laloi C, Minkov IN, Shulaev V, Apel K, Inzé D, Mittler R, Van Breusegem F. 2006. Transcriptomic footprints disclose specificity of reactive oxygen species signaling in Arabidopsis. *Plant Physiology* **141,** 436–445.

Gallego SM, Pena LB, Barcia RA, Azpilicueta CE, Iannone MF, Rosales EP, Zawoznik MS, Groppa MD, Benavides MP. 2012. Unravelling cadmium toxicity and tolerance in plants: Insight into regulatory mechanisms. *Environmental and Experimental Botany* **83,** 33–46.

Gandin A, Denysyuk M, Cousins AB. 2014. Disruption of the mitochondrial alternative oxidase (AOX) and uncoupling protein (UCP) alters rates of foliar nitrate and carbon assimilation in *Arabidopsis thaliana*. *Journal of Experimental Botany* **65,** 3133–3142.

Giraud E, Ho LHM, Clifton R, *et al*. 2008. The absence of ALTERNATIVE OXIDASE1a in Arabidopsis results in acute sensitivity to combined light and drought stress. *Plant Physiology* **147,** 595–610.

Heyno E, Klose C, Krieger-Liszkay A. 2008. Origin of cadmium-induced reactive oxygen species production: mitochondrial electron transfer versus plasma membrane NADPH oxidase. *New Phytologist* **179,** 687–699.

Jakubowicz M, Gałgańska H, Nowak W, Sadowski J. 2010. Exogenously induced expression of ethylene biosynthesis, ethylene perception, phospholipase D, and Rboh-oxidase genes in broccoli seedlings. *Journal of Experimental Botany* **61,** 3475–3491.

Jiang C, Belfield EJ, Cao Y, Smith JAC, Harberd NP. 2013. An *Arabidopsis* soil- salinity-tolerance mutation confers ethylene-mediated enhancement of sodium/potassium homeostasis. *The Plant Cell* **25,** 3535–3552.

Jozefczak M, Keunen E, Schat H, Bliek M, Hernández LE, Carleer R, Remans T, Bohler S, Vangronsveld J, Cuypers A. 2014. Differential response of *Arabidopsis* leaves and roots to cadmium: Glutathione-related chelating capacity *vs* antioxidant capacity. *Plant Physiology and Biochemistry* **83,** 1–9.

Keunen E, Jozefczak M, Remans T, Vangronsveld J, Cuypers A. 2013. Alternative respiration as a primary defence during cadmium-induced mitochondrial oxidative challenge in *Arabidopsis thaliana*. *Environmental and Experimental Botany* **91,** 63–73.

Keunen E, Truyens S, Bruckers L, Remans T, Vangronsveld J, Cuypers A. 2011. Survival of Cd-exposed *Arabidopsis thaliana*: are these plants reproductively challenged? *Plant Physiology and Biochemistry* **49,** 1084–1091.

Lei XY, Zhu RY, Zhang GY, Dai YR. 2003. Possible involvement of the mitochondrial alternative pathway in ethylene-induced apoptosis in tomato protoplasts. *Plant Growth Regulation* **41,** 111–116.

Li CR, Liang DD, Li J, Duan YB, Li H, Yang YC, Qin RY, Li L, Wei PC, Yang JB. 2013. Unravelling mitochondrial retrograde regulation in the abiotic stress induction of rice *ALTERNATIVE OXIDASE 1* genes. *Plant, Cell and Environment* **36,** 775–788.

Millar AH, Whelan J, Soole KL, Day DA. 2011. Organization and regulation of mitochondrial respiration in plants. *Annual Review of Plant Biology* **62,** 79–104.

Pasqualini S, Paolocci F, Borgogni A, Morettini R, Ederli L. 2007. The overexpression of an alternative oxidase gene triggers ozone sensitivity in tobacco plants. *Plant, Cell and Environment* **30,** 1545–1556.

Purvis AC, Shewfelt RL. 1993. Does the alternative pathway ameliorate chilling injury in sensitive plant tissues? *Physiologia Plantarum* **88,** 712–718.

Queval G, Noctor G. 2007. A plate reader method for the measurement of NAD, NADP, glutathione, and ascorbate in tissue extracts: Application to redox profiling during *Arabidopsis* rosette development. *Analytical Biochemistry* **363,** 58–69.

R Development Core Team. 2011. *R: A language and environment for statistical computing*. Vienna, Austria: R Foundation for Statistical Computing.

Remans T, Opdenakker K, Smeets K, Mathijsen D, Vangronsveld J, Cuypers A. 2010. Metal-specific and NADPH oxidase dependent changes in lipoxygenase and NADPH oxidase gene expression in *Arabidopsis thaliana* exposed to cadmium or excess copper. *Functional Plant Biology* **37,** 532–544.

Remans T, Smeets K, Opdenakker K, Mathijsen D, Vangronsveld J, Cuypers A. 2008. Normalisation of real-time RT-PCR gene expression measurements in *Arabidopsis thaliana* exposed to increased metal concentrations. *Planta* **227,** 1343–1349.

Sandalio LM, Dalurzo HC, Gómez M, Romero-Puertas MC, del Río LA. 2001. Cadmium-induced changes in the growth and oxidative metabolism of pea plants. *Journal of Experimental Botany* **52,** 2115–2126.

Schellingen K, Van Der Straeten D, Vandenbussche F, Prinsen E, Remans T, Vangronsveld J, Cuypers A. 2014. Cadmium-induced ethylene production and responses in *Arabidopsis thaliana* rely on *ACS2* and *ACS6* gene expression. *BMC Plant Biology* **14,** 214.

Sharma SS, Dietz KJ. 2009. The relationship between metal toxicity and cellular redox imbalance. *Trends in Plant Science* **14,** 43–50.

Smeets K, Ruytinx J, Van Belleghem F, Semane B, Lin D, Vangronsveld J, Cuypers A. 2008. Critical evaluation and statistical validation of a hydroponic culture system for *Arabidopsis thaliana*. *Plant Physiology and Biochemistry* **46,** 212–218.

Strodtkötter I, Padmasree K, Dinakar C, *et al*. 2009. Induction of the AOX1D isoform of alternative oxidase in *A. thaliana* T-DNA insertion lines lacking isoform AOX1A is insufficient to optimize photosynthesis when treated with antimycin A. *Molecular Plant* **2,** 284–297.

Sweetlove LJ, Heazlewood JL, Herald V, Holtzapffel R, Day DA, Leaver CJ, Millar AH. 2002. The impact of oxidative stress on *Arabidopsis* mitochondria. *The Plant Journal* **32,** 891–904.

Vandesompele J, De Preter K, Pattyn F, Poppe B, Van Roy N, De Paepe A, Speleman F. 2002. Accurate normalization of real-time

quantitative RT-PCR data by geometric averaging of multiple internal control genes. *Genome Biology* doi:10.1186/gb-2002-3-7-research0034

Vanlerberghe GC. 2013. Alternative oxidase: A mitochondrial respiratory pathway to maintain metabolic and signaling homeostasis during abiotic and biotic stress in plants. *International Journal of Molecular Sciences* **14,** 6805–6847.

Vanlerberghe GC, Cvetkovska M, Wang J. 2009. Is the maintenance of homeostatic mitochondrial signaling during stress a physiological role for alternative oxidase? *Physiologia Plantarum* **137,** 392–406.

Wang H, Liang X, Huang J, Zhang D, Lu H, Liu Z, Bi Y. 2010. Involvement of ethylene and hydrogen peroxide in induction of alternative respiratory pathway in salt-treated *Arabidopsis* calluses. *Plant and Cell Physiology* **51,** 1754–1765.

Watanabe CK, Hachiya T, Terashima I, Noguchi K. 2008. The lack of alternative oxidase at low temperature leads to a disruption of the balance in carbon and nitrogen metabolism, and to an up-regulation of antioxidant defence systems in *Arabidopsis thaliana* leaves. *Plant, Cell and Environment* **31,** 1190–1202.

Xu F, Yuan S, Zhang DW, Lv X, Lin HH. 2012. The role of alternative oxidase in tomato fruit ripening and its regulatory interaction with ethylene. *Journal of Experimental Botany* **63,** 5705–5716.